Design and Application of Coupled Line Cross-Shaped Resonator in Band-pass Filter

Dong-Sheng La [1,2], Xin Guan [1], Hong-Cheng Li [1], Yu-Ying Li [1], and Jing-Wei Guo [3]

[1] School of Computer and Communication Engineering
Northeastern University at Qinhuangdao, Qinhuangdao, 066004, China
ladongsheng@163.com, guanxinww@163.com, redorangel@163.com, believerr@163.com

[2] Guangxi Key Laboratory of Wireless Wideband Communication and Signal Processing
Guilin, 541004, China

[3] School of Information Science and Engineering
Yanshan University, Qinhuangdao, 066004, China
jingweiguo@ysu.edu.cn

Abstract ─ A coupled line cross-shaped resonator (CLCSR) is proposed, which consists of four parallel coupled lines. By using even- and odd-mode approach, this resonator is characterized and designed to build up a wide band-pass filter. There are three transmission poles in the pass-band and two transmission zeros out of the pass-band. The positions of the transmission zeros are fixed. The transmission poles are determined and adjusted by the parameters: z_1, z_2, k_1, and k_2. Then two coupled line cross-shaped resonators are cascaded to realize a wide band-pass filter. The sharper selectivity and better performance can be obtained by cascading two CLCSRs. Good S-parameters are achieved as demonstrated in both simulated and measured results.

Index Terms ─ Band-pass filter, coupled line cross-shaped resonator, transmission pole, transmission zero.

I. INTRODUCTION

The multi-mode resonator wide band-pass filter (BPF) design has become a research hotspot due to its simple filter topology, compact physical size and simple design process. In Ref. [1], an ultra-wideband BPF is designed with a cross-shaped resonator. An ultra-wideband BPF with the capacitively coupled stub-loaded resonator is introduced in Ref. [2]. Reference [3] proposes a differential wideband BPF which consists of slot-line multimode resonators. Cheng proposes a wideband BPF with reconfigurable bandwidth function [4]. The wideband BPF is composed of a parallel-coupled line structure and a cross-shaped resonator. In Refs. [5-11], some structures are added to the cross-shaped resonator, such as coupled lines, short stubs. Those band-pass filters provide better ideas for this study. There are many studies based on cross-shaped resonators. However, the performance of the ordinary cross-shaped resonators is poor, and the frequency selectivity of the filters needs to be improved.

In this paper, a new coupled line cross-shaped resonator filter is proposed. The input impedance of its equivalent circuit can be calculated through the odd-even mode method. The proposed filter is miniaturized by bending parallel coupled lines. In order to increase the bandwidth and improve the out-of-band performance, two CLCSRs are cascaded in the wideband BPF design. The simulated results are basically consistent with the measured ones. Compared with single cross-shaped resonator, the frequency selectivity of the cascaded CLCSR BPF is improved.

II. BAND-PASS FILTER DESIGN

Figure 1 (a) shows the proposed BPF which is composed of single CLCSR. The CLCSR consists of four parallel coupled lines. They are connected at the middle node position. The proposed BPF circuit is a symmetric structure. The odd mode characteristic impedance and even mode characteristic impedance of the parallel coupled lines are denoted as $z_{ce1} = z_1\sqrt{1+k_1}/\sqrt{1-k_1}$, $z_{co1} = z_1\sqrt{1-k_1}/\sqrt{1+k_1}$. The odd mode characteristic impedance and even mode characteristic impedance of the other two coupled lines are denoted as $z_{ce2} = z_2\sqrt{1+k_2}/\sqrt{1-k_2}$, $z_{co2} = z_2\sqrt{1-k_2}/\sqrt{1+k_2}$. The electrical length of all coupled lines is θ.

The odd mode circuit is shown in Fig. 1 (b) and the even mode circuit is shown in Fig. (c). The normalized impedance parameters $z_1 = Z_1/Z_0$ and $z_2 = Z_2/Z_0$ are

Submitted On: January 17, 2020
Accepted On: April 18, 2020

used in the even-odd mode circuit. The input impedances $z_{ine(o)}$ can be derived from formula (1) and (2) in Ref [12]. According to the odd-even mode circuit, the even mode load impedance is in formula (2) and the odd mode load impedance is in formula (3):

$$z_{ine(o)} = \frac{z_{Le(o)} z_1 (1-k_1^2) - (1-k_1^2) \tan\theta z_{Le(o)} z_1 + j z_1^2 \tan\theta \sqrt{1-k_1^2}}{(2j \tan\theta z_{Le(o)} \sqrt{1-k_1^2} + z_1(1+k_1))(1-k_1)}, \quad (1)$$

$$z_{Le} = \frac{z_2 \sqrt{1-k_2^2}}{2j \tan(\theta)(1-k_2)}, \quad (2)$$

$$z_{Lo} = 0. \quad (3)$$

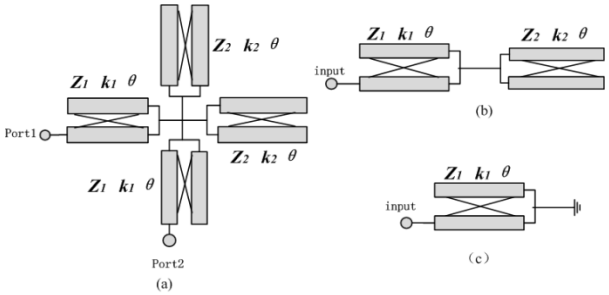

Fig. 1. (a) Ideal circuit of the CLCSR BPF, (b) odd-mode equivalent circuit, and (c) even-mode equivalent circuit.

In a symmetric two-port network, the normalized frequency response is

$$s_{11} = s_{22} = \frac{z_{ine} z_{ino} - 1}{(z_{ine} - 1)(z_{ino} - 1)}, \quad (4)$$

$$s_{12} = s_{21} = \frac{z_{ine} - z_{ino}}{(z_{ine} - 1)(z_{ino} - 1)}. \quad (5)$$

When θ is equal to π, the corresponding frequency is f_0, as shown in formula (6). When $|s_{21}|$ is equal to zero, the transmission zeros of the CLCSR BPF can be obtained. The transmission zeros f_{z1} and f_{z2} are shown in formula (7a) and (7b). The positions of the CLCSR BPF's transmission zeros can be adjusted through the f_0:

$$\theta = \pi = \frac{2\pi f_0}{v} l, \quad (6)$$

$$f_{z1} = \frac{1}{2} f_0, \quad (7a)$$

$$f_{z2} = \frac{3}{2} f_0. \quad (7b)$$

When $|s_{11}|$ is equal to zero, the transmission poles of the CLCSR BPF can be obtained. The calculated results of the transmission poles are as shown in formula (8) and (9):

$$f_{p1} = \frac{2 f_0 \arctan(\sqrt{u_p})}{\pi}, \quad (8)$$

$$f_{p2} = f_0, \quad (9)$$

$$f_{p3} = \frac{2 f_0 (\pi - \arctan(\sqrt{u_p}))}{\pi}, \quad (10)$$

$$u_p = \frac{(-\sqrt{1-k_1^2} z_2 (-\frac{1}{2} z_1^2 + k_1 - 1)\sqrt{1-k_2^2} + z_1 (k_1^2 - 1)(k_2 - 1))(1+k_1)}{z_1^2 (-\frac{1}{2} z_2 (-1+k_1)\sqrt{1-k_2^2}\sqrt{1-k_1^2} - z_1 (1+k_1)(k_2 - 1))}. \quad (11)$$

The transmission poles f_{p1} and f_{p3} are symmetric about the f_0. There are two transmission zeros out of the pass-band and three transmission poles in the pass-band. The zero-pole distribution of the ideal CLCSR BPF is shown in Fig. 2.

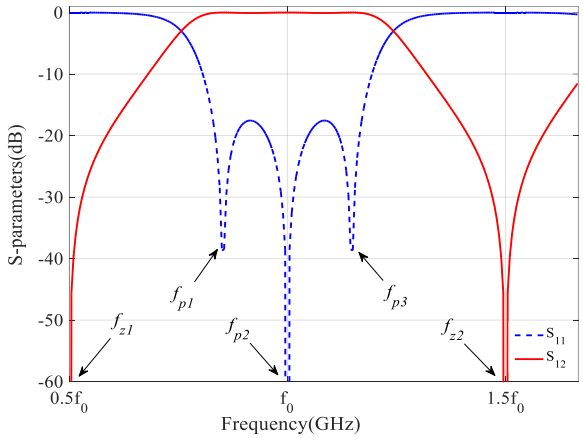

Fig. 2. Zero-pole distribution of the CLCSR BPF's circuit.

In Fig. 2, the relationship between the transmission poles and the transmission zeros in the frequency range is:

$$f_{z1} < f_{p1} < f_{p2} < f_{p3} < f_{z2}. \quad (12)$$

The influence of the design parameters on the return loss of the CLCSR BPF is given in Fig. 3. When one parameter changes, the other parameters remain unchanging. The transmission poles f_{p1} and f_{p3} are far away from each other when one parameter increases. In Fig. 3 (a), with the increases of k_1, the return loss decreases and the frequency selectivity is improved. The bandwidth increases and the return loss decreases with the increases of k_2 in Fig. 3 (b). In Fig. 3 (c), the frequency selectivity is improved and the return loss decreases with the increase of z_1. In Fig. 3 (d), the bandwidth increases and the return loss decreases with the increase of z_2.

The physical structure parameters of the coupled lines

can be calculated based on Z and k. The characteristic impedance Z is smaller when the width of the coupled line is wider. When the gap between the coupled lines is wider, the value of k is usually smaller. Thus, the design parameters are selected as $k_1 = k_2 = 0.6$, $z_1 = z_2 = 1.5$.

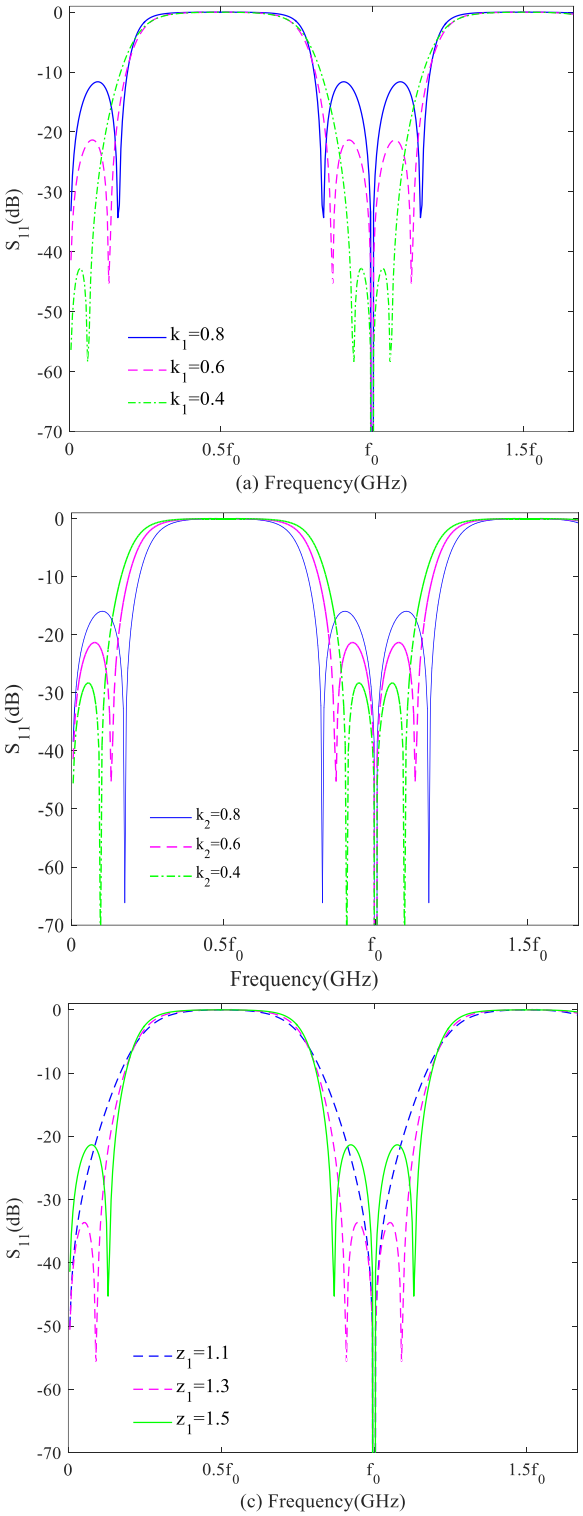

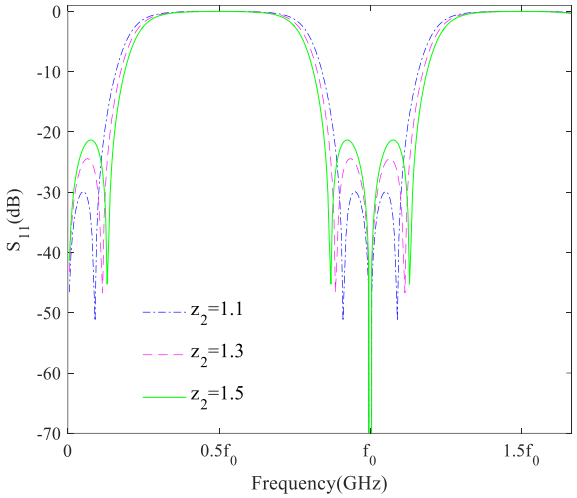

Fig. 3. The influence of z_1, z_2, k_1, and k_2 on the return loss of the CLCSR BPF: (a) z_1; (b) z_2; (c) k_1; (d) k_2.

III. RESULT AND DISCUSSION

The final size of the CLCSR BPF is shown in Fig. 4 (a) and the photograph of the CLCSR BPF is shown in Fig. 4 (b).The coupled lines are bended for filter miniaturization. The resonant frequencies of the CLCSR BPF are simulated by using ANSYS HFSS. The EM method in simulation is finite element method. The CLCSR BPF is designed on Rogers RT5880 microwave dielectric board (h = 0.508 mm, $\varepsilon_{re} = 2.2$, $\tan\delta = 0.0009$). The line width g=1.54*mm* is chosen for the characteristic impedance of 50Ω for the input/output microstrip line. The characteristic impedance of SMA connector is 50Ω which matches the microstrip line.

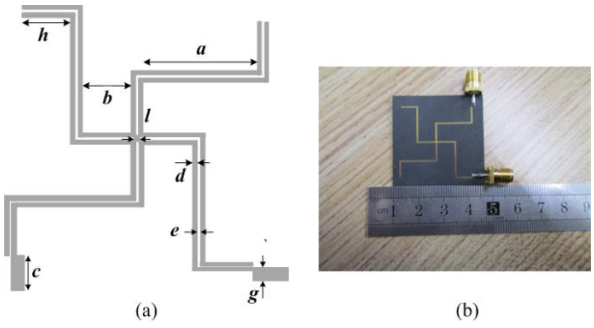

Fig. 4. (a) The CLCSR BPF structure parameters (*a*=14.1, *b*=7.19, *c*=5, *d*=0.255, *e*=0.15, *g*=1.54, *h*=6.58, *l*=0.2, Unit: *mm*), (b) photograph of the CLCSR BPF.

Figure 5 shows the simulated and measured results of the CLCSR BPF. The measured results are obtained with Agilent N5230C vector network analyzer. As shown in Fig. 5, the measured results almost agree well with the simulation ones. The absolute bandwidth of the CLCSR BPF is 1.6 GHz, which is from 3.2 to 4.8 GHz. The return

loss is bigger than 12dB in the whole pass-band. In addition, the stop-band rejection is better than 14dB from 2 to 3.2 GHz. Moreover the stop-band rejection is better than 12 dB from 4.8 to 7 GHz.

In order to improve the out-of-band performance and expand the pass-band frequency range, two CLCSRs are cascaded in wide-band BPF design. Figure 6 (a) shows the equivalent circuit of the cascaded CLCSR BPF. The cascaded CLCSR BPF structure parameters are slightly different from the CLCSR BPF in Fig. 1. The cascaded CLCSR BPF layout is shown in Fig. 6 (b) and the photograph of the cascaded CLCSR BPF is shown in Fig. 6 (c).

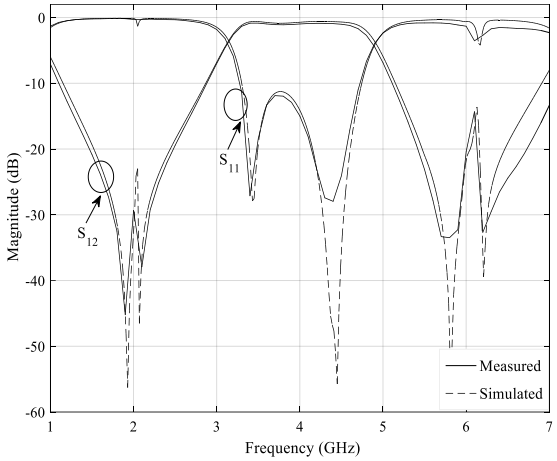

Fig. 5. Simulated and measured results of the CLCSR BPF.

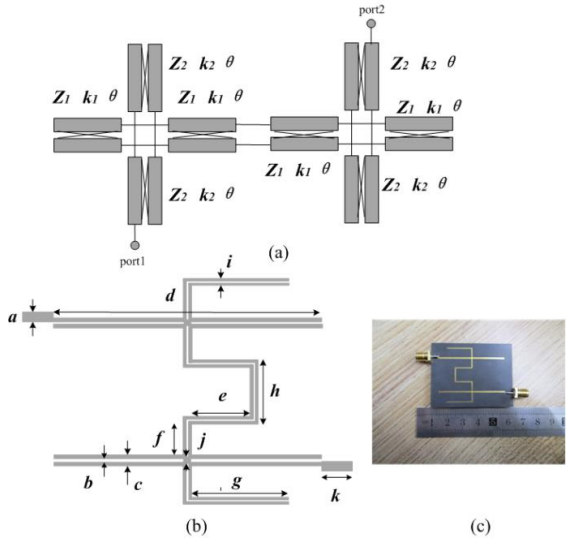

Fig. 6. (a) Ideal circuit diagram for the cascaded CLCSR BPF, (b) actual size of the cascaded CLCSR BPF circuit (*a=1.54, b=0.15, c=1.05, d=43.12, e=10.78, f=5.92, g=16.66, h=4.9, i=0.7, j=0.2, k=4.5, Unit: mm*), (c) photograph of the cascaded CLCSR BPF.

The simulated and measured results of the cascaded CLCSR BPF are shown in Fig. 7. The absolute bandwidth of the cascaded CLCSR BPF is 2 GHz from 4.2 to 6.2 GHz. The return loss is bigger than 12dB in the pass-band. The out-of-band rejection levels are greater than 20 dB. The simulated results are basically consistent with the measured ones. The frequency discrepancy between the simulated and measured results is due to the machining error and the material parameters difference. The material parameters include the dielectric constant and the thickness of dielectric plate. The discrepancy of the return loss and the insertion loss is due to the conductor loss, the dielectric loss and the radiation loss. There are a few errors in the simulated and measured results, which also makes the simulated results different from the measured ones.

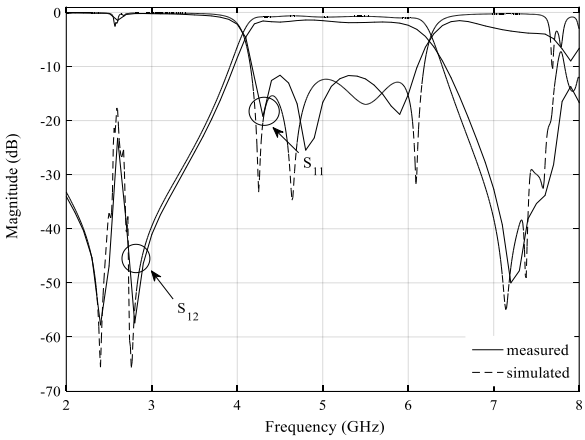

Fig. 7. Simulated and measured results of the cascaded CLCSR BPF.

Table 1 compares the proposed works with some previous works. Obviously, the proposed filters have some advantages, such as wide bandwidth, compact size and high performance.

IV. CONCLUSION

In this paper, a CLCSR is proposed, which consists of four parallel coupled lines. By using the odd-even mode method, the CLCSR is analyzed and designed to construct a wide-band BPF. The cascaded CLCSR BPF is designed by cascading CLCSRs. Finally, the CLCSR BPF and the cascaded CLCSR BPF are simulated, fabricated and measured. The simulated and measured results for two proposed wide-band BPFs are basically the same.

ACKNOWLEDGMENT

This work is supported by National Natural Science Foundation of China under Grant 61501100, Natural Science Foundation of Hebei Province under Grant F2019203012, the Fundamental Research Funds for the

Central Universities under Grant N2023017, and the Open Project of Guangxi Key Laboratory of Wireless Wideband Communication and Signal Processing under Grant GXKL06180201.

Table 1: Compares the proposed works with some previous works

Reference	Center Frequency	TZs/TPs	Insertion Loss	Return Loss	Size ($\lambda_g * \lambda_g$)
Ref. [1]	6.65	2/4	0.35	>20	0.5*0.79
Ref. [2]	6.85	4/5	0.6	>14	0.38*1.14
Ref. [3]	2.6	Not give	0.5	>10	1.4*1.4
Ref. [4]	5.7	2/3	1.4	>10	0.18*0.18
Ref. [5]	1.75	Not give	1.5	Not give	0.38*0.17
CLCSR BPF	4	2/3	0.4	>12	0.15*0.15
Cascaded CLCSR BPF	5.2	2/5	1.1	>12	0.19*0.15

REFERENCES

[1] H. Wang, G. Yang, and W. Kang, "Application of cross-shaped resonator to the ultra wideband bandpass filter design," *IEEE Microwave and Wireless Components Letters*, vol. 17, no. 12, pp. 667-669, Dec. 2011.

[2] T. H. Duong and I. S. Kim, "Steeply sloped UWB band-pass filter based on stub-loaded resonator," *IEEE Microwave and Wireless Components Letters*, vol. 20, no. 8, pp. 441-443, Aug. 2010.

[3] D. Chen, H. Z. Bu, L. Zhu, et al., "A differential-mode wideband band-pass filter on slot-line multi-mode resonator with controllable bandwidth," *IEEE Microwave and Wireless Components Letters*, vol. 25, no. 1, pp. 28-30, Jan. 2015.

[4] T. Cheng and K. W. Tam, "A wideband band-pass filter with reconfigurable bandwidth based on cross-shaped resonator," *IEEE Microwave and Wireless Components Letters*, vol. 27, no. 10, pp. 909-911, Oct. 2017.

[5] A. Zakharov and M. Ilchenko, "Trisection micro-strip delay line filter with mixed cross-coupling," *IEEE Microwave and Wireless Components Letters*, vol. 27, no. 12, pp. 1083-1085, Dec. 2017.

[6] X. K. Bi, C. Teng, P. Cheong, et al., "Wideband band-pass filters with reconfigurable bandwidth and fixed notch bands based on terminated cross-shaped resonator," *IET Microwaves, Antennas & Propagation*, vol. 13 no. 6, pp. 796-803, May 2019.

[7] Z. C. Guo, L. Zhu, and S. W. Wong, "A quantitative approach for direct synthesis of band-pass filters composed of transversal resonators," *IEEE Transactions on Circuits and Systems—II: Express Briefs*, vol. 66, no. 4, pp.577-581, Apr. 2019.

[8] D. Chen, H. Z. Bu, L. Zhu, et al., "A differential-mode wideband band-pass filter on slot-line multi-mode resonator with controllable bandwidth," *IEEE Microwave and Wireless Components Letters*, vol. 25, no. 1, pp. 28-30, Jan. 2015.

[9] L. X. Zhou, Y. Z. Yin, W. Hu, et al., "Compact band-pass filter with sharp out-of-band rejection and its application," *ACES Journal*, vol. 32, no. 3, pp. 249-255, Mar. 2017.

[10] M. Y. Fu, Q. Y. Xiang, and Q. Y. Feng, "A tunable trisection bandpass filter with constant fractional bandwidth based on magnetic coupling," *ACES Journal*, vol. 34, no. 12, pp. 1888-1896, Dec. 2019.

[11] D. Y. Tian, Q. Y. Feng, and Q. Y. Xiang, "Design of high order cross-coupled constant absolute bandwidth frequency-agile bandpass filters," *ACES Journal*, vol. 34, no. 9, pp. 1373-1378, Sep. 2019.

[12] I. Z. George and A. K. Johnson, "Coupled transmission line networks in an inhomogeneous dielectric medium," *IEEE Transactions on Microwave Theory and Techniques*, vol. 17, no. 10, pp. 753~759, Oct. 1969.

Dong-Sheng La was born in Hebei, P.R. China. He has received his Masters degrees from Xinjiang Astronomical Observatory, Chinese Academy of Sciences in 2008, and his Ph.D. degrees from Beijing University of Posts and Telecommunications in 2011. He is currently an Associate Professor in the School of Computer and Communication Engineering, Northeastern University at Qinhuangdao in China. His recent research interests include passive RF components, patch antennas and electromagnetic compatibility. He has authored or coauthored over 20 journal and conference papers.

Xin Guan received B.S. degree in Information Warfare Technology from Shenyang Ligong University, Shenyang, China, in 2018. Since 2018, she is now working toward the Master degree in Northeastern University at Qinhuangdao, Qinhuangdao, China, where she

studied the content of electromagnetic waves, microstrip transmission lines, and microstrip filters. Her research interests include microwave filter, electromagnetic compatibility.

Hong-Cheng Li received the Bachelor's degree in Communications Engineering from Northeastern University at Qinhuangdao, Qinhuangdao, China, in 2019. He is now working toward the Master degree in Northeastern University, Qinhuangdao, China. His research interests include synthesis and design of microwave filters, electromagnetic compatibility.

Yu-Ying Li received the Bachelor's degree in Electronic Information Engineering from Shenyang University of Technology, Shenyang, China, in 2019. She is now working toward the Master degree in Northeastern University at Qinhuangdao, Qinhuangdao, China. Her research interests include antenna and antenna array.

Jing-Wei Guo was born in Hebei, China, in 1982. He received his Ph.D. degree in Electromagnetic Field and Microwave Technology from Beijing University of Posts and Telecommunications in 2011. He is engaging in the research of metamaterials, semiconductor technology and optoelectronic field recently, as an Associate Professor of Yanshan University, China.